ELSEVIER

Biophysical Chemistry 57 (1996) 155-161

Biophysical Chemistry

Local analysis of the M state kinetics of bacteriorhodopsin

E. Papp *, Viet Hien Ha

Department of Atomic Physics, Eötvös University, Puskin u. 5, Budapest H-1088, Hungary

Received 5 September 1994; revised 16 May 1995; accepted 26 May 1995

Abstract

Two kinetic models (A and B) of the photocycle of bacteriorhodopsin are analyzed around the M state and compared with experimental kinetic absorption data measured at 410 nm. Both models assume two isospectral M states: M_1 and M_2. Model A is a sequential allowing back reaction between the L and M_1 intermediate states. Model B has a branching after L to M_1 and M_2. Solving the first order reaction differential equations it is shown that both models result in the same time dependence for the transient absorption change at 410 nm ($M_1 + M_2$ intermediate states). This time functional form describes well the experimental data. Though the two models cannot be distinguished on the basis of the functional form alone. But fitting to the experimental data gives acceptable parameters for model B; for model A we get unacceptable results.

Keywords: Bacteriorhodopsin; Photocycle; Sequential; Branching

1. Introduction

Bacteriorhodopsin (BR) is an integral membrane protein in the purple membrane (PM) of *Halobacterium halobium*. A retinal molecule is attached to Lys-216 side chain through a Schiff base. Absorbing a photon the retinal and the protein undergo a complex change, the photocycle. After excitation BR returns to the initial state through thermally activated intermediate states: J, K, L, M, N, O, with characteristic absorption bands and lifetimes. During the photocycle the Schiff base is transiently deprotonated and later reprotonated, which results in a proton translocation through the membrane (for recent reviews see e.g. [1,2]).

Different kinetic models have been proposed for the photocycle. One of the first, [3], took into account sequential, unidirectional steps between the intermediate states. The apparent biphasic rise and decay of the M state observed in kinetic absorption measurements was interpreted by a branching in the photocycle [4–8]. The possibility of parallel photocycles was also taken into account [9,10]. From kinetic Raman and FTIR study results a single sequential photocycle was proposed with back reactions between some of the intermediates [11,12]. To account for the observation that the concentration of the L intermediate goes to zero while M is high, despite of the quasi-equilibrium between L and M, two sequential, but isospectral M substates, (M_1 and

---

* Corresponding author.

SSDI 0301-4622(95)00074-7

M_2, where M_1 decays irreversibly into M_2), were assumed [13]. The main problem in the interpretation of the spectroscopic data is that there are many intermediates and there is a strong overlap between their spectra [14]. The only exception is the M state, whose absorption band is separated from the others.

We found that the time course of the measured transient absorption change at 410 nm (M intermediate state) can be represented well with the following function:

$$A(t) = g_1(e^{-g_3 t} - e^{-g_2 t}) + g_4(e^{-g_5 t} - e^{-g_2 t}) + \text{const.} \qquad (1)$$

This function describes a biphasic decay of the M state, g_1 and g_4 are amplitudes and g_2 (build-up), g_3 and g_5 (decay) are apparent rate constants for build-up and decay.

At least two kinetic reaction models can lead to the absorption change described by Eq. (1). One is a sequential model with back reaction between the L and M_1 states, assuming two isospectral M substates which are connected by an irreversible step (model A). The other kinetic model leading to the same absorption (Eq. (1)) is a branching model. Assuming again two isospectral M substates, the branching is at the decay of the L state (model B).

In the following we solve the reaction differential equations for both models and show that both models lead to the same absorption time dependence, given by Eq. (1). We compare the experimental data measured at 410 nm with both models.

2. Materials and methods

The PM suspensions isolated from *Halobacterium halobium* strain S9 were gifts from the Biophysics Institute, Biological Research Center, Szeged, Hungary. Concentrated suspensions were diluted in distilled water to an optical density of 3 at 575 nm and light-adapted before measurements. Absorption change of the M state was measured at 410 nm by a photomultiplier. For the monitor light we used a halogen lamp of 50 W and a set of colored glass and interference filters. For excitation of the photocycle a Nd-YAG laser (Quanta-Ray GCR-130, Spectra-Physics, USA), frequency doubled to 530 nm, was applied with a pulse duration of 6–8 ns and pulse energy of 1 mJ at the sample, and the light pulse was positioned perpendicularly to the monitoring beam. The anode current of the photomultiplier was digitalized by a DC coupled digital storage adaptor (DSA-524, Thurlby-Thandard Ltd., England) and stored in an AT386 desk-top computer. The data were averaged over 128 traces. The measuring temperatures were 20, 25, 30 and 35°C.

The experimental data were fitted to Eq. (1) by using a nonlinear least square fit [15], modified and called Curfit10.

3. Results

3.1. Reversible photocycle (model A)

First we analyze and solve the following reaction chain (model A):

$$L \underset{k_2}{\overset{k_1}{\rightleftharpoons}} M_1 \overset{k_3}{\rightarrow} M_2 \overset{k_4}{\rightarrow} .$$

Here it is assumed that there are two different, but isospectral M states (M_1 and M_2). The reaction between L and M_1 is reversible with rate constants k_1 and k_2, but the reaction between M_1 and M_2 is irreversible with a rate constant of k_3. The differential equations for these reactions:

$$\frac{dL}{dt} = -k_1 L + k_2 M_1$$
$$\frac{dM_1}{dt} = k_1 L - (k_2 + k_3) M_1 \qquad (3)$$
$$\frac{dM_2}{dt} = k_3 M_1 - k_4 M_2 .$$

Introducing a vector $\underline{x} = (x_1, x_2, x_3)$ for the three states L, M_1 and M_2, Eq. (3) can be written as a matrix equation:

$$\dot{\underline{x}} = K\underline{x} \qquad (4)$$

where K is the following (3 × 3) matrix:

$$K = \begin{pmatrix} -k_1 & k_2 & 0 \\ k_1 & -(k_2 + k_3) & 0 \\ 0 & k_3 & -k_4 \end{pmatrix} . \qquad (5)$$

The general solution of differential equations (3) can be given in terms of the eigenvectors and eigenvalues of the matrix K [16]. If λ_i and $\underline{y}^i$ are the eigenvalues and eigenvectors of the matrix K, then the general solution to Eq. (3) is:

$$\underline{x}(t) = \sum_{i=1}^{3} c_i e^{\lambda_i t} \underline{y}^i. \qquad (6)$$

The constants c_i are determined by the initial conditions, for which we assume:

$$\begin{aligned} &\mathrm{L}(0) = a \quad x_1(0) = a \\ &\mathrm{M}_1(0) = 0 \quad x_2(0) = 0 \\ &\mathrm{M}_2(0) = 0 \quad x_3(0) = 0. \end{aligned} \qquad (7)$$

(It means that we assume that the initial steps in the photocycle are much faster than the lifetimes of the L and M states.)

As in the third column of the matrix K there is only one nonzero element, the eigenvalue problem is simplified. We get for $\lambda_3 = -k_4$ and for the other two eigenvalues the following second order equation:

$$(k_1 + \lambda)(k_2 + k_3 + \lambda) - k_1 k_2 = 0. \qquad (8)$$

Eq. (8) has the following solutions:

$$\lambda_{1,2} = \frac{1}{2}\left[-(k_1 + k_2 + k_3) \pm |k_1 + k_2 - k_3| \times \sqrt{1 + \frac{4k_2k_3}{(k_1 + k_2 - k_3)^2}} \right]. \qquad (9)$$

As we expect that k_1 is at least an order of magnitude larger than k_3, we expand the square root in Eq. (9). In this approximation we get for the eigenvalues:

$$\begin{aligned} \lambda_1 &= -(k_1 + k_2 + \Delta) \\ \lambda_2 &= -k_3 + \Delta \\ \lambda_3 &= -k_4 \end{aligned} \qquad (10)$$

where

$$\Delta = k_2 k_3/(k_1 + k_2 - k_3).$$

For the eigenvectors, $\underline{y}^i$, we get the following result:

$$\underline{y}^1 = \left(-\frac{k_2}{k_2 + \Delta}, 1, -\frac{k_3}{k_1 + k_2 - k_4 + \Delta} \right)$$

$$\underline{y}^2 = \left(\frac{k_2 + \Delta}{k_1}, 1, -\frac{k_3}{k_3 - k_4 - \Delta} \right)$$

$$\underline{y}^3 = (0, 0, 1). \qquad (11)$$

The general solution of the differential Eqs. (3,4) is given with Eq. (6):

$$\begin{aligned} x_1(t) &= c_1 e^{\lambda_1 t} y_1^1 + c_2 e^{\lambda_2 t} y_1^2 \\ x_2(t) &= c_1 e^{\lambda_1 t} + c_2 e^{\lambda_2 t} \\ x_3(t) &= c_1 e^{\lambda_1 t} y_3^1 + c_2 e^{\lambda_2 t} y_3^2 + c_3 e^{\lambda_3 t}. \end{aligned} \qquad (12)$$

The constants, c_i, are determined by the initial conditions, Eq. (7):

$$\begin{aligned} c_1 &= a/(y_1^1 - y_1^2) \\ c_2 &= -c_1 \\ c_3 &= c_1(y_3^2 - y_3^1). \end{aligned} \qquad (13)$$

As M_1 and M_2 are isospectral, the absorption change at 410 nm will be determined by the sum of these two substates. This is given by Eq. (14).

$$\begin{aligned} x_2(t) + x_3(t) = {} & c_1\left(1 + \frac{k_3}{k_4 + \lambda_1}\right) e^{\lambda_1 t} \\ & - c_1\left(1 + \frac{k_3}{k_4 + \lambda_2}\right) e^{\lambda_2 t} \\ & + c_1\left(\frac{k_3}{k_4 + \lambda_2} - \frac{k_3}{k_4 + \lambda_1}\right) e^{-k_4 t}. \end{aligned} \qquad (14)$$

Eq. (14) has the same form as Eq. (1). It is important to note that for the amplitudes of the exponentials in Eq. (14) the same relation is fulfilled as in Eq. (1), because we have:

$$\begin{aligned} c_1\left(1 + \frac{k_3}{k_4 + \lambda_1}\right) = {} & c_1\left(1 + \frac{k_3}{k_4 + \lambda_2}\right) \\ & + c_1\left(\frac{k_3}{k_4 + \lambda_1} - \frac{k_3}{k_4 + \lambda_2}\right). \end{aligned} \qquad (15)$$

Both Eqs. (1) and (14) have the same number of parameters and a unique relation can be given between them.

3.2. Branching photocycle (model B)

Next we solve the differential equations for the branching photocycle (model B):

$$\begin{array}{cccc} & k_1 & & k_3 \\ & \nearrow & M_1 & \rightarrow \\ L & & & \\ & \searrow & M_2 & \rightarrow . \\ & k_2 & & k_4 \end{array}$$

The differential equations for these reactions are given by Eq. (16).

$$\frac{dL}{dt} = -(k_1 + k_2)L$$
$$\frac{dM_1}{dt} = k_1 L - k_3 M_1 \qquad (16)$$
$$\frac{dM_2}{dt} = k_2 L - k_4 M_2 .$$

Though differential Eqs. (16) are much simpler than Eqs. (3) and could be solved directly, we follow the general method given above, using the same notation. The matrix K for these reactions is given by Eq. (17).

$$K = \begin{pmatrix} -(k_1 + k_2) & 0 & 0 \\ k_1 & -k_3 & 0 \\ k_2 & 0 & -k_4 \end{pmatrix}. \qquad (17)$$

Eq. (18) gives the eigenvalues of this K matrix.

$$\lambda_1 = -(k_1 + k_2)$$
$$\lambda_2 = -k_3$$
$$\lambda_3 = -k_4 . \qquad (18)$$

The eigenvectors of the K matrix are given by Eq. (19).

$$\underline{y}^1 = \left(1, -\frac{k_1}{k_1 + k_2 - k_3}, -\frac{k_2}{k_1 + k_2 - k_4}\right)$$
$$\underline{y}^2 = (0, 1, 0)$$
$$\underline{y}^3 = (0, 0, 1). \qquad (19)$$

The general solution of the differential Eqs. (16):

$$x_1(t) = c_1 e^{\lambda_1 t}$$
$$x_2(t) = c_1 e^{\lambda_1 t} y_2^1 + c_2 e^{\lambda_2 t}$$
$$x_3(t) = c_1 e^{\lambda_1 t} y_3^1 + c_3 e^{\lambda_3 t}. \qquad (20)$$

Again the constants, c_i, are determined by the initial conditions given by Eq. (7):

$$c_1 = a$$
$$c_2 = -c_1 y_2^1$$
$$c_3 = -c_1 y_3^1 . \qquad (21)$$

The absorption change at 410 nm is determined by the sum of the two M substates, for which we get from Eq. (20) the following result:

$$x_2(t) + x_3(t) = a\frac{k_1}{k_1 + k_2 - k_3}\left(e^{\lambda_2 t} - e^{\lambda_1 t}\right) + a\frac{k_2}{k_1 + k_2 - k_4}\left(e^{\lambda_3 t} - e^{\lambda_1 t}\right). \qquad (22)$$

Again Eq. (22) has the same form and time dependence as Eq. (1). Both equations have the same number of parameters and a unique relation can be given between them.

4. Discussion

It was shown above that both local photocycle models A and B lead to the same time dependence of the absorption change at 410 nm, given by Eq. (1). Just on the ground of time dependence of the absorption change, these models cannot be distinguished. But these models are not equivalent, behind them the molecular events during the photocycle should be quite different. So it is important to compare these models further.

We carried out transient absorption change measurements on PM at 410 nm in a range of temperature and pH. All measured absorptions were fitted to Eq. (1) using the nonlinear least square fit program, Curfit10. Fig. 1 shows one of these measurements and the result of the fit.

The fit yields five parameters $g_1, \ldots, g_5$. As there is a unique relation between Eq. (1) and the final results of models A and B (Eq. (14) and Eq. (22)), the five g_i parameters can be converted to the five kinetic parameters $(a, k_1, \ldots, k_4)$ of the models A and B.

For model B we always got acceptable kinetic parameters (e.g. all are positive). An Arrhenius plot

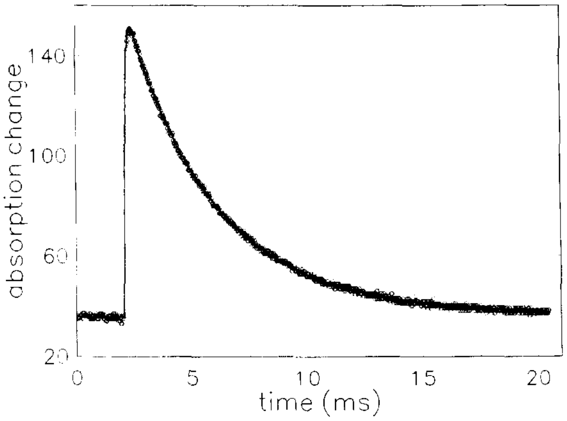

Fig. 1. Transient absorption changes measured at 410 nm (circles) and the fit to Eq. (1) (solid line). (PM in distilled water, pH = 7.4, 25°C).

for the four rate constants is shown in Fig. 2. Rate constants k_1 and k_3 are not sensitive to pH changes and show linear Arrhenius behavior. Rate constants k_2 and k_4 show larger scattering, deviations from the linear in the Arrhenius plot and stronger temperature and pH dependence.

For model A the kinetic parameters derived from the g_i parameters were in the examined cases in some sense not acceptable. For rate constant k_2 we get negative values, for rate constants k_1 and k_2 the values are too high (higher than 10^5 s^{-1}) and the amplitude, a, varies strongly with temperature,

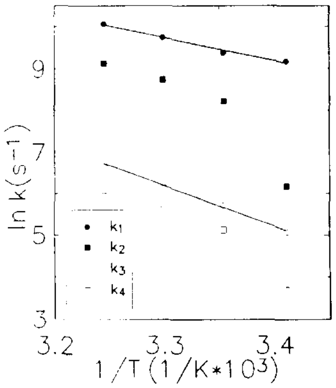

Fig. 2. Arrhenius plot of the four rate constants of model B. (PM in distilled water, pH = 7.4).

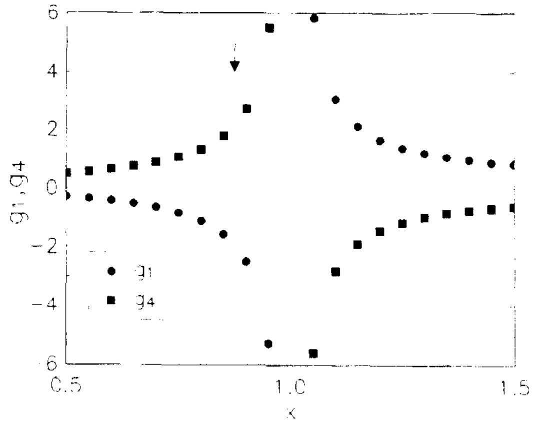

Fig. 3. The dependence of the two amplitudes on parameter x. (x is given by Eq. (23)).

though the exciting laser pulse energy (and so the quantity of the excited BR) was rather stable.

It is interesting to note that model A kinetics are represented in Eq. (1) with amplitudes g_1 and g_4 of opposite signs. To show this we took approximate numerical values for model A from Ref. 17 ($k_1 = 2.98 \cdot 10^4$; $k_2 = 6.72 \cdot 10^4$; $k_3 = 1.87 \cdot 10^4$; $k_4 = 2.88 \cdot 10^2$ s^{-1} and for the amplitude in Eq. (7) we assumed $a = 1$). We converted $(k_1, \ldots, k_4, a)$ to $(g_1, \ldots, g_5)$ of Eq. (1). But for a more general behavior we varied the parameter x in a range (by varying k_4), as the g_1, g_4 amplitudes depend strongly on x. The parameter x is given by Eq. (23).

$$x = \frac{k_2}{k_1 + k_2 - k_3} + \frac{k_4}{k_3}. \tag{23}$$

The behavior of g_1, g_4 is shown in Fig. 3. As can be seen g_1 and g_4 are always opposite in sign. The arrow shows the actual value for the kinetic parameters taken from Ref. 17. The problem is again that from experimental data fitting to Eq. (1) we always got positive values for g_1 and g_4.

The initial conditions given in Eq. (7) are approximations, which may affect the above results. We made the following numerical simulation to check the effect of the initial conditions. First, with the initial conditions of Eq. (7), we generated a data file (very similar to the measured data given in Fig. 1) using Eq. (14) and the above given kinetic parameters taken from Ref. 17. These generated data were fitted to Eq. (1) by using our Curfit10 program, which yielded the following values: $g_1 = -1.90$; $g_2 = 1.13 \cdot 10^5\ s^{-1}$; $g_3 = 2.66 \cdot 10^3\ s^{-1}$; $g_4 = 2.14$; $g_5 = 2.88 \cdot 10^2\ s^{-1}$ (for g_1 and g_4 see also Fig. 3, too). These g- parameters can be converted to the kinetic parameters of model A and B. Model A returns the starting values with high precision but model B gives unphysical results (among others negative k_1 in Eq. (22)), indicating that model B does not work with a data set generated by model A. To account for a finite transition rate between K and L (or KL [18] and L), we took a Gaussian distribution around $t = 0$ as the initial condition for the intermediate state L. With nine components, distributed under the Gaussian curve (one at $t = 0$, four before and four after $t = 0$) we calculated the function given by Eq. (14) separately with the same kinetic parameters but delayed by the proper time interval. After calculation we added the nine components with amplitude weights according to the Gaussian curve. This data set was fitted again to Eq. (1) by Curfit10. The effect of increasing the half width of the Gaussian curve is mainly the decrease of the apparent rate constant g_2, the other four parameters do not change. E.g. a 5-μs half-width gives: $g_1 = -1.9$; $g_2 = 1.09 \cdot 10^5\ s^{-1}$; $g_3 = 2.66 \cdot 10^3$; $g_4 = 2.14$; $g_5 = 2.88 \cdot 10^2\ s^{-1}$. (The experimentally observed lifetime of K is around 1.5 μs at the given temperature [17]). According to this simulation we believe that the assumed initial conditions (Eq. (7)) are not responsible for the problems encountered with model A.

We did the same simulation starting with model B kinetics (Eq. (22)). The result was similar to the above discussed model A calculation. A data set generated by model B yields such fitting parameters $g_1, \ldots, g_5$ which, after conversion to model A, results in negative k_2, but the conversion to model B returns the starting values for the kinetic parameters. The initial conditions with Gaussian distribution have much less effects for model B kinetics.

This local analysis supports better the branching model B. Global analysis of the photocycle (see e.g. Refs. [2,14,17,19]) is very important, but it supports the sequential, reversible kinetics between L and M_1. As we pointed out in this paper a local analysis contradicts the global analysis around the M states. We think that more work is needed to understand theses different results in global and local analyses.

We restricted our consideration to kinetic models A and B and we do not go into any detail of the possible molecular events behind these models. We would only like to make the remark that the existence of two primary proton acceptors to the Schiff base would result in a model B type branching in the photocycle. We emphasize that this problem arose in connection with our measurements of proton release and uptake. We found that the proton release (and uptake) is a biphasic process which can be accounted for by the existence of a second primary acceptor to the Schiff base. We proposed Asp-212 for the second primary acceptor. Related considerations will be given elsewhere in connection with proton release and uptake measurements [20].

Acknowledgements

We thank the Biophysics Institute of the Hungarian Academy of Sciences and Dr. J. Heberle for providing PM preparations. This work was supported by the Hungarian Science Foundation grant 914.

References

[1] R.A. Mathies, S.W. Lin, J.B. Ames and W.T. Pollard, Annu. Rev. Biophys. Biophys. Chem., 20 (1991) 491.

[2] J.K. Lanyi, Biochem. Biophys. Acta, Bioenerg. Rev., 1183 (1993) 241.

[3] R.H. Lozier, R.A. Bogomolni and W. Stoeckenius, Biophys. J., 15 (1975) 955.

[4] W.V. Sherman, R.R. Eicke, S.R. Stafford and F.M. Wasacz, Photochem. Photobiol., 30 (1979) 727.

[5] Q.Q. Li, R. Govindjee and T. Ebrey, Proc. Natl. Acad. Sci. USA, 81 (1984) 7079.

[6] J.M. Beach and R.S. Fager, Photochem. Photobiol., 41 (1985) 557.

[7] G. Fricsovszky, E. Papp, G. Meszéna and A. El-Lakkani, Stud. Biophys., 111 (1986) 23.

[8] T. Kouyama, A. Nasuda-Kouyama, A. Ikegami, M.K. Mathew and W. Stoeckenius, Biochemistry, 27 (1988) 5855.

[9] J.H. Hanamoto, P. Dupuis and M.A. El-Sayed, Proc. Natl. Acad. Sci. USA, 81 (1984) 7083.

[10] Z. Dancsházy, R. Govindjee and T.G. Ebrey, Proc. Natl. Acad. Sci. USA, 85 (1988) 6358.

[11] K. Gerwert, G. Souvignier and B. Hess, Proc. Natl. Acad. Sci. USA, 87 (1990) 9774.

[12] J.B. Ames and R.A. Mathies, Biochemistry, 29 (1990) 7181.
[13] Gy. Váró and J.K. Lanyi, Biochemistry, 30 (1991) 5008.
[14] J.F. Nagle, Biophys. J., 59 (1991) 476.
[15] P.R. Bevington, Data Reduction and Error Analysis for the Physical Sciences, Mc Graw-Hill, New York, 1969.
[16] J.J. Tyson, in S. Levin (Editor), Biomathematics, The Belousov-Zhabotinskii reaction, Vol. 10, Springer-Verlag, Berlin, 1976.
[17] G. Váró and J.K. Lanyi, Biochemistry, 30 (1991) 5016.
[18] S.J. Milder and D.S. Kliger, Biophys. J., 53 (1988) 465.
[19] L. Zimányi and J.K. Lanyi, Biophys. J., 64 (1993) 240.
[20] E. Papp and V.H. Ha, J. Photochem. Photobiol. B: Biology, in press.